Short period holographic structures for backlight display applications

Roberto Caputo, Luciano De Sio, Martin J.J. Jak, Eefje J. Hornix, Dick K.G. de Boer and Hugo J. Cornelissen

Philips Research Europe, High Tech Campus 34, 5656AE Eindhoven, The Netherlands

Abstract: The use of holographic structures is promising for the realization of efficient systems in backlight applications for displays. By applying surface relief gratings on top of a side-lit lightguide we realize a backlight that avoids the use of color filters. The grating is used as a light outcoupling and color-separating element. The demands for this grating are stringent and calculations have been performed to meet them. A prototype backlight, including the grating structure, has been assembled and characterized. Results of experiments are discussed.

OCIS codes: (050.7330) Volume holographic gratings; (220.4830) Optical systems design; (330.1710) Color measurement

References and links

1. S. Serak, N. Tabiryan and B. Zeldovich, "High-efficiency 1.5 μm thick optical axis grating and its use for laser beam combining," Opt. Lett. **32**, 169-171 (2007).
2. X. Wang, D. Wilson, R. Muller, P. Maker and D. Psaltis, "Liquid-crystal blazed-grating beam deflector," Appl. Opt. **39**, 6545-6555 (2000).
3. D. Wright, E. Brasselet, J. Zyss, G. Langer and W. Kern, "Dye-doped organic distributed-feedback lasers with index and surface gratings: the role of pump polarization and molecular orientation," J. Opt. Soc. Am. B **21**, 944-950 (2004).
4. R. Jakubiak, L.V. Natarajan, V. Tondiglia, G. S. He, P. N. Prasad, T. J. Bunning and R. A. Vaia, "Electrically switchable lasing from pyrromethene 597 embedded holographic-polymer dispersed liquid crystals," Appl. Phys. Lett. **85**, 6095 (2004).
5. M.-C. Oh, K.-J. Kim, J.-H. Lee, H.-X. Chen, and K.-N. Koh, "Polymeric waveguide biosensors with calixarene monolayer for detecting potassium ion concentration," Appl. Phys. Lett. **89**, 251104 (2006).
6. J. W. Kang, M. J. Kim, J. P. Kim, S. J. Yoo, J. S. Lee, D. Y. Kim, and J J. Kim "Polymeric wavelength filters fabricated using holographic surface relief gratings on azobenzene-containing polymer films," Appl. Phys. Lett. **82**, 3823 (2003).
7. C. Sánchez, M. J. Escuti, C. van Heesch, C. W. M. Bastiaansen and D. J. Broer, "An efficient illumination system for liquid crystal displays incorporating an anisotropic hologram," Appl. Phys. Lett. **87**, 094101 (2005).
8. Y. Taira, D. Nakano, H. Numata, A. Nishikai, S. Ono, F. Yamada, M. Suzuki, M. Noguchi, R. Singh, E. G. Colgan, "Low-power LCD using a novel optical system," SID 02 Digest 1313-1315 (2002); F. Yamada, S. Ono, Y. Taira, "Dual layered very thin flat surface micro prism array directly molded in an LCD cell," Eurodisplay 2002, 339-342 (2002).
9. D. K. G. de Boer, R. Caputo, H. J. Cornelissen, C. M. van Heesch, E. J. Hornix, M. J. J. Jak "Diffractive grating structures for colour-separating backlights," Proc. SPIE **6196**, 241 (2006).
10. M. Xu, H. P. Urbach and D. K. G. de Boer, "Simulations of birefringent gratings as polarizing color separator in backlight for flat-panel displays," Opt. Express **15**, 5789 (2007).
11. Y-S. Choi, J-S. Choi, J-H. Min, J-H. Kim, S-M. Lee, "Backlight unit for flat panel display and flat panel display apparatus having the same," U.S. patent application publication US2006/0285185 (Dec. 21, 2006).
12. Grating solver development company. www.gsolver.com
13. M. G. Moharam and T. K. Gaylord, "Rigorous coupled-wave analysis of planar-grating diffraction," J. Opt. Soc. Am. **71**, 811 (1981).

#84201 - $15.00 USD Received 18 Jun 2007; revised 2 Aug 2007; accepted 2 Aug 2007; published 6 Aug 2007

14. AZ Electronic Materials. www.az-em.com
15. ELDIM manufacturer of 2D photometers & colorimeters and Inspection systems. www.eldim.fr

1. Introduction

In the last few years, a lot of attention has been devoted to the realization of new devices based on holographic diffractive structures. These diffractive elements can be implemented in many configurations. The amount of possibilities is quite vast including beam steering devices [1,2], organic lasers [3,4], smart sensors [5] and wavelength selective filters[6], lighting and display systems [7]. In the last case, usually waveguides are used in which light propagates by means of total internal reflection (TIR). If a grating is accurately designed and integrated in the waveguide, a precise control of the light extraction process can be achieved. In this paper we consider the design and realization of a high quality short-pitched diffraction grating used for improving the efficiency of backlit displays. The light management in present liquid crystal displays (LCDs) is not very efficient: only a small percentage (~4-6%) of the light generated in the backlight of the device reaches the eyes of the user. One of the main challenges in display research is the realization of systems optimized for reducing power consumption. An innovative way for achieving this result has been proposed by Taira et al., [8] who demonstrated how the color-dispersion power of a diffraction grating can be efficiently employed to avoid the use of color filters. Since the percentage of light absorbed in these filters can be estimated to be 65-70%, there could be a considerable advantage in designing and adopting diffractive structures for display applications. The grating separates the incoming light into fundamental colors with different angles. The obtained light rays impinge on a microlens array that properly redirects the colors to the pixels of the LCD. A similar approach was taken by De Boer et al., [9] who applied the grating directly on top of a lightguide (Fig. 1).

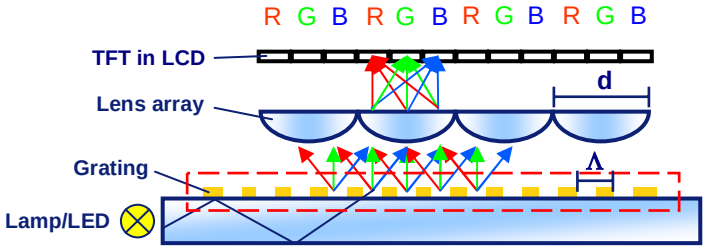

Fig. 1. Color-filterless display configuration including a grating structure. The grating on top of a lightguide separates incoming light into red, green and blue colors. A lens array put in front of the grating images the various beams on the LC layer forming an RGB pixel structure. The figure is not to scale: the pitch of the grating is of the order of visible wavelengths, $\Lambda \approx 400$nm while the pitch of the lens array is $d \approx 800\mu$m.

In another work by Xu *et al*. [10], a birefringent grating was considered and the advantages of polarized outcoupling were studied.

2. Design of a grating for a backlight system

If a grating is considered for backlight applications, its design must fulfill several conditions in order to obtain a working device. As a starting point, we can assume that the lamp illuminating the side facet of the light guide emits light in a Lambertian (cosine) way. In case we have a PMMA light guide (refractive index n=1.5), the light rays coming from the lamp will be refracted at the entrance facet of the guide and will then propagate with angles restricted to the interval ±42° with respect to the normal to the facet. This implies that these rays make angles between 48° and 90° with the normal to the grating (Fig. 2). Without grating the light is simply captured inside the light guide by total internal reflection (TIR). In the

#84201 - $15.00 USD Received 18 Jun 2007; revised 2 Aug 2007; accepted 2 Aug 2007; published 6 Aug 2007

presence of the grating we expect that the light is partly diffracted and partly reflected back into the guide. The number of diffraction orders in which it is coupled out depends on the grating properties. In order to realize the configuration of Fig. 1, it is preferable that all the light that is incident on the grating is diffracted in a single order and angularly separated depending on the wavelengths present in its spectrum.

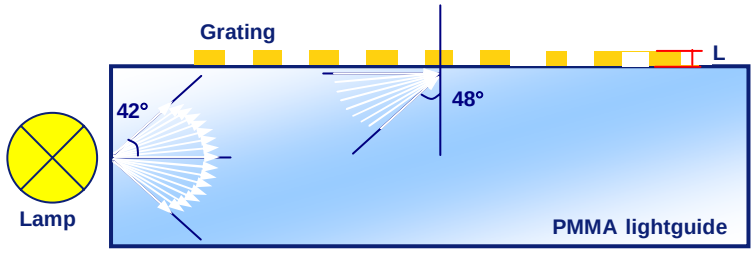

Fig. 2. Light propagating inside the lightguide is restricted to angles of ±42° with the normal to the entrance facet of the guide due to refraction. The light rays that are incident on the grating will make angles between 48° and 90° with the normal to its surface. Due to the Lambertian intensity distribution of light entering the lightguide, light incident on the grating with small angles (close to 48°) is less intense than light incident with steeper angles (close to 90°).

The conditions necessary for obtaining this result can be calculated by using the grating equation:

$$m\lambda = \Lambda(n_2 \sin\theta_{dif} - n_1 \sin\theta_{inc}) \quad (1)$$

Here, λ is the wavelength of the light, m is an integer number corresponding to the considered diffraction order, Λ is the period of the grating, n_1 is the refractive index of the light guide, θ_{inc} is the angle formed by the beam incoming on the grating with its normal and θ_{dif} is the angle formed instead by the m^{th} diffracted beam. For diffraction into air (light transmitted, T) n_2=1, for diffraction into the lightguide (light reflected, R) n_2=n_1. By using Eq. (1), we can determine the number of diffraction orders that are coupled out from the structure and what the diffracted angles are. In Fig. 3, we show the behavior for three different values of Λ (700nm, 500nm, 300nm) and three values of the wavelength λ of the incoming beam (615nm, 545nm, 450nm). The choice of short periods in the calculations is aimed to obtain a good angular separation between various colors. For what concerns the wavelengths, they represent typical peak values in the spectral range of a CCFL (cold-cathode fluorescence lamp) lamp commonly used in backlights. Instead, LEDs emitting around these wavelengths could be used.

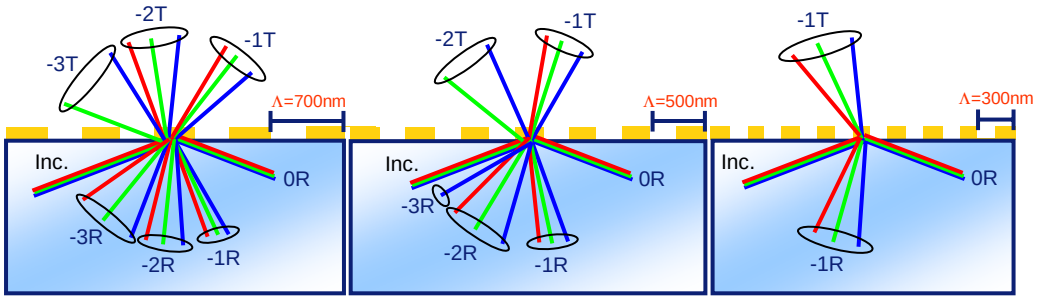

Fig. 3. Estimation of the number of diffraction orders coupled out by a diffraction grating and of angles that they form with the normal to it for different periods (700nm, 500nm, 300nm). In all cases the same incidence angle θ_{inc}=69° is considered.

#84201 - $15.00 USD Received 18 Jun 2007; revised 2 Aug 2007; accepted 2 Aug 2007; published 6 Aug 2007

For the sake of simplicity, in all cases shown in Fig. 3 the incident angle is θ_{inc}=69° because it corresponds to the central value of the cone of incident angles (48°<θ_{inc}<90°). In the Figure, mT and mR (m=0,-1,-2,-3..), respectively, indicate the transmitted and reflected diffracted orders. Results clearly show that it is possible to achieve a single diffracted transmitted order, for all wavelengths, by using gratings with a very short period (Λ<500nm). For this period, the only other order still present is the -1R. In order to avoid light losses, it is preferable to put a reflective layer underneath the lightguide to recycle this contribution. From Fig. 3, we can also deduce that, by slightly changing the period of the grating, we can control the width of the angular region spanned by the outcoupled colors and which angles they form with the grating normal. When dealing with backlight systems, an important parameter of the device is the homogeneity of the light intensity over the illuminated area. Because in our system light comes from the grating, this feature depends on the properties of the grating. The ability of a grating to outcouple light can be measured by its diffraction efficiency (DE). The efficiency of a given diffraction order is defined as the ratio between the intensity of the order and that of the light incident on the grating. By relating the spatial distribution of the extracted light to the DE of the grating, we can obtain a useful information for the design of our grating. In the configuration of Fig. 1 we assume that light propagates in the light guide bouncing up and down inside it. If, for example, the DE of the grating is very low, we guess that, at every "bounce" of light on the grating surface, just a small portion of the incident light will be coupled out. This gives a quite uniform intensity distribution along the guide but our device can also be very inefficient: all the light which arrives at the end facet of the guide and has not yet been coupled out exits from the lightguide and hence is lost. By placing a mirror at the end of the light guide, we can prevent this situation. In contrast, if the DE is very high, a large amount of light is coupled out at the beginning of the guide, close to the lamp, leaving just a small portion for the remaining part. The obtained light intensity distribution along the guide will in this case be very asymmetric which is undesirable. A third possibility is that of increasing the DE of the grating along the lightguide [11]. In this way, by moving away from the light source, the decreasing intensity of light can be compensated with a larger extraction efficiency. This result can be obtained by varying the grating depth along the guide. The realization of such a grating is however quite difficult to obtain. We can conclude that, depending on the size of the backlight that we want to realize, the simplest solution is to find a tradeoff value for the DE. Finally, it is also important to remember that the light entering the guide has a Lambertian intensity distribution. For geometrical reasons, we expect that light coming to the grating with small angles with the normal (Fig. 2, angles close to 48°) is less intense than light incident with steeper ones (Fig. 2, angles close to 90°). This means that the shape of the DE curve versus the incidence angle θ_{inc} for the wavelengths of interest is also very important. In particular, if the DE curve shows a monotonously decreasing behavior for increasing angle, the grating can compensate the Lambertian distribution of the light source giving similar intensities for all diffracted angles. It is also desirable that the DE curve has a smooth behavior, without anomalies, so that there are no angles in some way "privileged" by the outcoupling process. In order to take into account all the considerations above and to obtain a reliable estimation of the design parameters for our grating, we performed several numerical simulations by using the commercially available GSolver software [12] that employs a rigorous coupled wave analysis (RCWA) [13]. Results of simulations performed in the past on similar systems [9] showed that the DE of the grating is strongly related to its depth L. For this reason, we calculated the behavior of the DE of the grating for the first diffraction order (sum of -1T and -1R) by varying the incidence angle θ_{inc} and the wavelength of the incident light λ for several L values. Gratings considered are restricted to rectangular ones with vertical side walls and duty cycle of 50% (percentage of the period occupied by the photoresist material). The obtained results are summarized in the contour plots of Fig. 4. The diffraction efficiency is plotted versus the incidence angle θ_{inc} and the wavelength λ. In every

#84201 - $15.00 USD Received 18 Jun 2007; revised 2 Aug 2007; accepted 2 Aug 2007; published 6 Aug 2007

column, the number above the plot indicates the depth L of the grating. The three rows of plots reported in Figs 4(a), 4(b), 4(c) show simulations for different periods of the grating, respectively, Λ=300nm, Λ=400nm, Λ=500nm. We did not extend simulations to values Λ>500nm because then there are several transmitted orders. These results depict a large range of grating behaviors. As discussed above, we wish to have a smooth, decreasing behavior of the DE simultaneously for all the wavelengths of interest (450nm<λ<650nm). By carefully observing Fig. 4, we can notice that this behavior is indeed realized when the grating depth is in some interval which depends on the period of the grating. These intervals are indicated on the left side of Fig. 4 by enclosing the corresponding graphs in red rectangles.

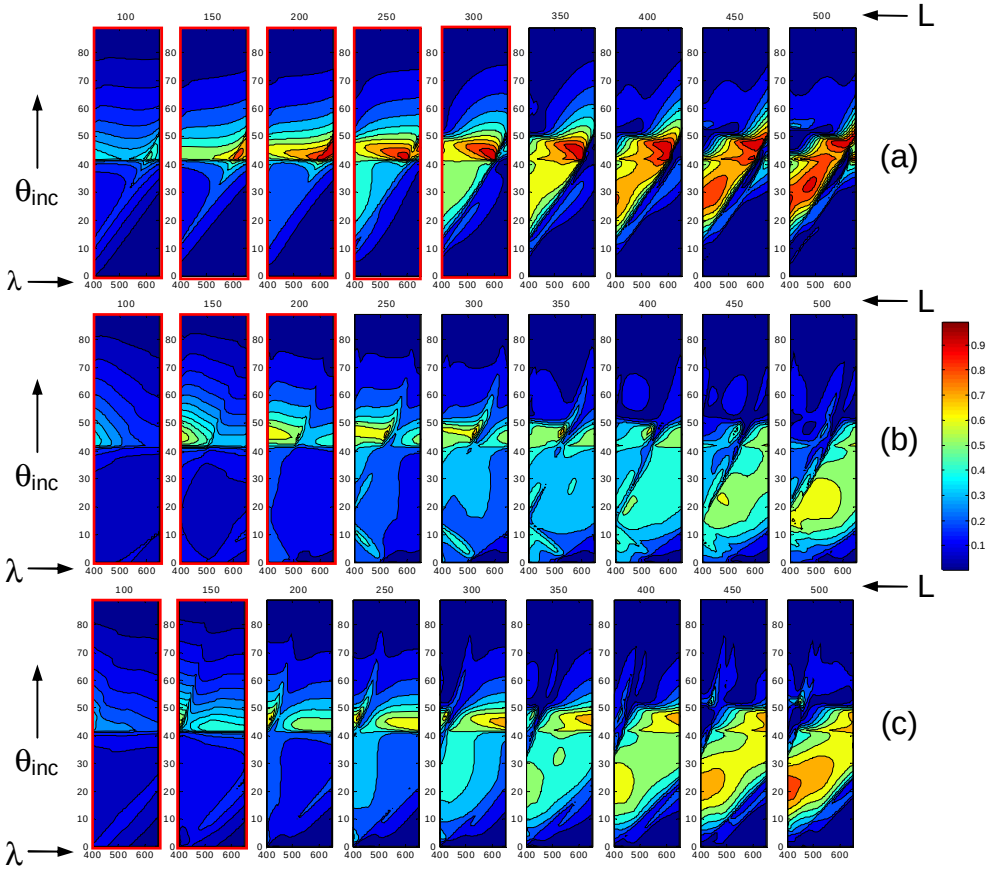

Fig. 4. Contour plots of the diffraction efficiency of the grating for the first diffraction order (sum of -1T and -1R) versus incidence angle θ_{inc} and wavelength λ. In a given row, the number above every plot indicates the depth L of the grating. (a) Λ=300nm; (b) Λ=400nm, (c) Λ=500nm. The red rectangles in the Figure indicate the intervals for the grating depth that gives a smooth, decreasing DE as function of incident angle simultaneously for all wavelengths of interest (450nm<λ<650nm).

2. Configuration of the backlight system

With the conditions obtained in the previous section for the period and the depth, we have restricted the range of possible grating parameters to some intervals of interest. The next step is to define the angular properties of the colored ray pattern, at the exit of the grating, that are suitable for obtaining a color filterless display. Once known, this ray configuration can be realized by fine tuning of the grating parameters. Our starting point is the geometry sketched in Fig. 1. In order to avoid efficiency issues (see considerations above) we can include a

#84201 - $15.00 USD Received 18 Jun 2007; revised 2 Aug 2007; accepted 2 Aug 2007; published 6 Aug 2007

reflector at the end of the light guide. Unfortunately, with the reflector another drawback immediately emerges. The light reflected at the end of the guide propagates with opposite direction with respect to that coming directly from the lamp. This counter-propagating light is also diffracted by the grating, but this time the angles of blue and red rays are reversed. This gives rise to a color-mixing effect that generates a magenta-green-magenta pixel structure on the LC layer. Hence this configuration (Fig. 1) can be used only with light coming from one side in order to maintain a proper separation of colors. A similar drawback is intrinsically present also in the configuration illustrated in [7]. In that case a slanted grating (e.g. a grating with fringes having an angle with respect to the grating normal) has been adopted to color-separate the light. If a mirror is included in that case at the end of the guide, the counter-propagating light will be diffracted by the slanted grating with a completely asymmetric angular pattern with respect to that relative to the propagating wave and in a wrong diffractive regime (no Bragg condition), resulting in an unwanted angular intensity distribution. An alternative configuration that can solve the color mixing problem is proposed in Fig. 5. In this new configuration, the light guide is illuminated from both sides and the grating period can be chosen in such a way to emit blue along the normal direction while green and red will be diffracted at larger angles. Thanks to this new geometry, the light that is extracted from the grating and comes from opposite directions adds up producing a symmetric red-green-blue-green-red pattern and avoiding the color-mixing. The lens array on top of the grating is four instead of three pixels wide and the width and strength of the lenses are chosen such that the red lines created by neighbouring lenses overlap. This creates a sequence of red – green – blue – green – red lines on the TFT matrix in the LC layer of the device. A diffuser foil can also be included in the system (between the lenses and the LC layer) in order to enlarge the viewing angle.

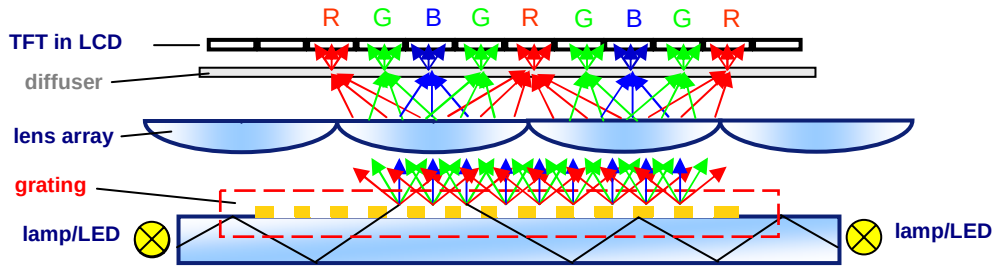

Fig. 5. Optimal backlight configuration. Light from opposite directions is diffracted by the grating and generates a symmetric RGBGR pattern which avoids color-mixing problems. The figure is not to scale: the pitch of the grating is of the order of visible wavelengths, $\Lambda \approx 400$nm while the pitch of the lens array is $d \approx 800\mu$m.

3. Experimental evaluation of a working prototype

The optical quality requirements for a grating in a display configuration are quite challenging. If we consider how strongly the diffraction efficiency depends on period and depth (Fig. 4), we easily understand that even small variations of these parameters would end up in optical defects for the display. Moreover, typical applications for an LCD display involve large areas (typically 42 inches for LCD-TV applications) and the grating should be as large as the display itself. In order to realize a grating with a very large area and high optical quality a refined industrial process is necessary. In our case, the main aim was to verify results of our simulations by realizing a working prototype. For this reason, we preferred a grating with a small area (typical for mobile applications) but with a high optical quality. The grating has been experimentally realized following the procedure depicted in Fig. 6(a). The first step (glass coating) consists of realizing a thin film of a photoresist material on a glass substrate. In our case, we deposited the AZ1518 [14] positive photoresist on the glass by spin coating. The

#84201 - $15.00 USD Received 18 Jun 2007; revised 2 Aug 2007; accepted 2 Aug 2007; published 6 Aug 2007

optical quality of the grating strongly depends on this step: it is fundamental to achieve a homogeneous film of controlled thickness all over the sample area. The next step (curing stage) concerns the writing of the grating in the photoresist-coated sample. A holographic experimental setup has been arranged for this purpose (Fig. 6(b)). A single mode beam from an Ar-ion laser operating at wavelength λ=363.8 nm is broadened by a spatial filter (composed by two lenses L1, L2, and a small aperture I) up to a diameter of about 30 mm. It is divided into two parts of nearly the same intensity by the polarizing beam splitter P. In order to have the same polarization of these two beams, a half-wave plate HWP has been placed in one of the two arms of the interferometer system. These two beams intersect at the entrance plane of the sample S, giving rise to an interference pattern made of high and low intensity stripes whose spatial period depends on the interference angle θ_c which is half the angle between the two beams.

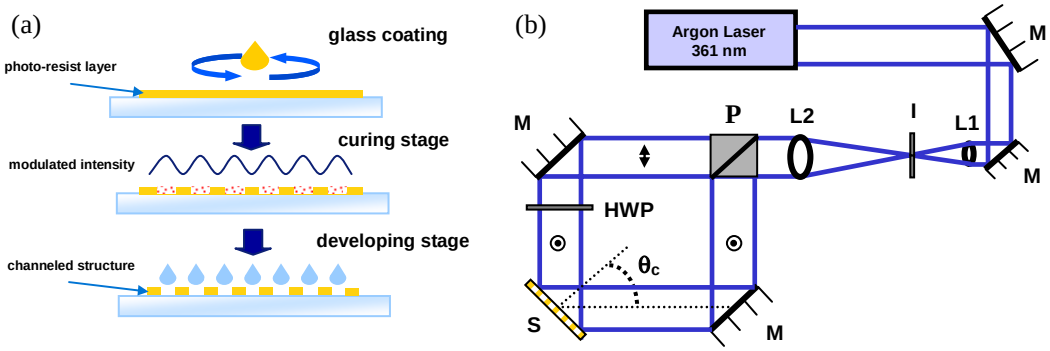

Fig. 6. (a). Sketch of the whole process for the realization of grating structures; (b) Optical setup for making the holographic gratings; M, mirrors; L1, L2, lenses; I, aperture; P, polarizer beam splitter; HWP, half-wave plate; θ_c, recording beam angle; S, sample.

The period of the grating can be easily changed by varying θ_c according to the formula:

$$\Lambda = \frac{\lambda}{2\sin\theta_c} \tag{2}$$

where Λ is the period of the grating and λ the wavelength of the curing beams. An important parameter to be considered when realizing periodic structures on photosensitive materials is the light energy absorbed by the material during exposure. This amount of energy is generally called dose (indicated with D) and it is related to the curing time t and curing power P, namely: D=P*t. By changing the dose, it is possible to control the depth of the obtained grating. In particular, by increasing it will result in deeper structures. An extremely high dose can completely erase all the photoresist material resulting in no grating at all. This case is defined as “over-exposure”. If the dose is very low, the photoresist layer remains instead practically untouched, corresponding to “under-exposure”. A value of the dose in between these two extremes will result in optimal structures. In order to state the dose values corresponding to under- and over-exposure, a series of gratings is generally prepared by starting writing with a low value of the dose and increasing it until a high one. The obtained samples are then analyzed at the scanning electron microscope (SEM) in such a way to relate the dose to the depth and morphological quality of the gratings. The final step is the development of the sample (developing stage): a solvent is used to remove the cured material inside the grating. By using this procedure, we have obtained very high quality structures free of optical defects even on large areas. In Fig. 7, a SEM micrograph of a typical structure is reported. The grating morphology is very regular. This fulfills the optical quality requirements we discussed above. The optimal period for the grating with blue (λ=450nm) along the normal

#84201 - $15.00 USD Received 18 Jun 2007; revised 2 Aug 2007; accepted 2 Aug 2007; published 6 Aug 2007

(θ_{dif}=0°) results from Eq. (1) and is given by Λ=320nm. This value fits very well with the condition for having a single diffracted transmitted order from the grating (Λ<500nm). We recall that the simulations implied that optimum values for the depth are 200nm<L<300nm. The grating period Λ=320nm can be obtained by fixing in the setup θ_c=34.64° (see Fig. 6(b)).

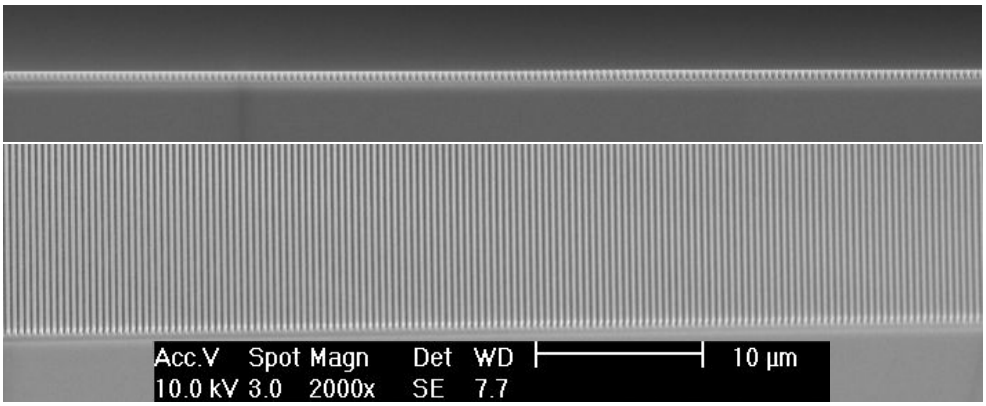

Fig. 7. SEM picture of a typical structure obtained by holographic techniques with photoresist materials. The structure is highly regular by observing the sample both in cross-section (a) and in top view (b).

A grating depth L=210nm has been achieved by illuminating the sample with a dose D=100µW*20sec=2000µJ. This particular dose value is the result of the empirical procedure described above. In particular, we fixed the power to the value where the laser showed a good stability (P=100µW) and then changed the exposure times for finding the optimal interval. The extreme values of this interval are obtained for times t_{low}=17sec. and t_{high}=25sec. which correspond to depth values for the grating of L_{lmin}≈120nm and L_{max}≈600nm, respectively. The SEM micrograph of the realized grating is shown in Fig. 8(a).

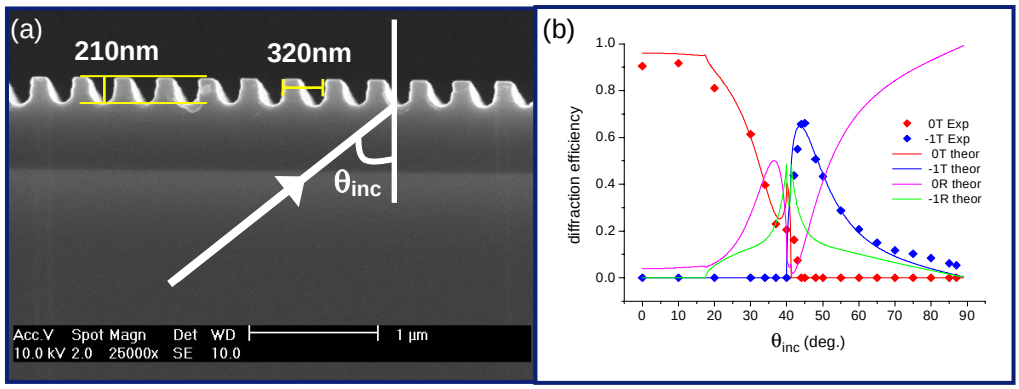

Fig. 8. (a). SEM picture of the realized grating structure. The fringe spacing is about Λ=320nm and the thickness of the grating about L=210nm; (b) diffraction efficiency plot of the realized grating. Dots indicate experimental measurements while solid lines (red and blue curves) are the GSolver fits for the same structure. Theoretical values of the intensities for the 0R and -1R orders (magenta and green curves respectively) are also reported as a reference.

#84201 - $15.00 USD Received 18 Jun 2007; revised 2 Aug 2007; accepted 2 Aug 2007; published 6 Aug 2007

In order to test the obtained grating before including it in the display structure, we measured its diffraction efficiency with a He-Ne laser (λ=632.8 nm) as a probe and compared the result with the GSolver simulation of the same structure (Fig. 8(b)). For the simulation we assumed a structure with same period and depth as the real grating and a rectangular refractive index profile with a duty cycle of 50%. The refractive index of the photoresist material has been estimated to be 1.6 for the wavelengths of interest. The agreement between experiment and simulation is quite satisfactory. By using the same simulation parameters, we also plotted the diffraction efficiency (only for the -1T order) for the three fundamental colors (615nm, 545nm, 450nm) versus diffraction angles produced by this grating (Fig. 9(a)). Gray curves show what would be the diffraction intensities of the various colors if there were no restrictions on the incident beam angles ($0°<\theta_{inc}<90°$). Dashed rectangles indicate the overlap regions between various colors. The presence of two colors in the same region possibly results in an issue for the color purity of the obtained device. This problem can be prevented by restricting the angular range of the light coming to the grating from the lightguide. In that case, the angular cones spanned by the various colors are reduced and the overlap regions are limited or completely avoided. In Fig. 9(b) a plot is shown of the diffraction angle (obtained from the grating Eq. (1)) that illustrates how the color overlap could be prevented by reducing the incidence interval to $62°<\theta_{inc}<90°$. As it is clearly visible in the Figure, in this case the angular ranges of the diffracted beams have no intersections at all. Collimation of the input light can be achieved by a funnel shaped entrance of the lightguide. In case LEDs are used as light source, reflective and/or refractive optics close to the LEDs are commonly used for such a purpose.

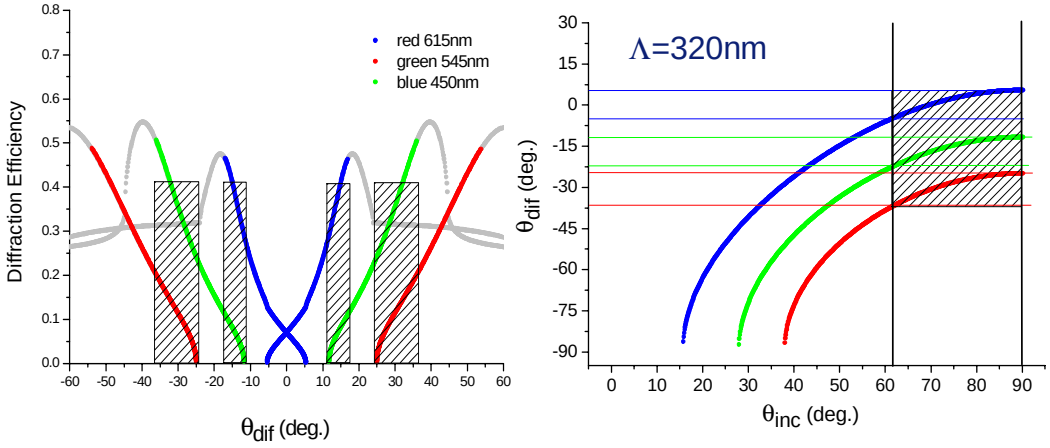

Fig. 9. (a). Plot of the diffraction efficiency versus diffracted angle. Colored curves show the outcoupled beams from the lightguide in a red-green-blue-green-red sequence. Gray curves represent the behavior of the grating when the incoming beams have no angular constraints (i.e. all incident angles occur). Dashed rectangles show the overlap regions between outcoupled colors. (b). Plot of the diffraction angle versus incident angle for a grating with a periodicity Λ=320nm.

In Fig. 8(b), the theoretical curves for the 0R and -1R orders (magenta and green curves respectively) have been included as a reference. It can be noticed that the DE value of the -1R order is also considerable in the angular range of interest ($48°<\theta_{inc}<90°$). In order to recycle this order and to avoid optical losses, a reflective layer has been imcluded underneath the lightguide. From Eq. (1), it can be seen that the -1R contributions reflected by this layer are transmitted by the grating into the same direction as the -1T order, for every angle belonging to $48°<\theta_{inc}<90°$ (Fig. 10). This is true for every wavelength propagating in the lightguide. One

#84201 - $15.00 USD Received 18 Jun 2007; revised 2 Aug 2007; accepted 2 Aug 2007; published 6 Aug 2007

may worry about the subsequent diffraction of the -1R rays reflected by the reflective layer. However, also from Eq. (1), it can be shown that these rays belong to an angular interval of incidence on the grating (e.g. $-23°<\theta_{-1R}<-8°$ for the green) where no transmitted diffracted orders (1T or -1T) are allowed by the chosen periodicity (Λ=320nm, see Fig. 9(b)). Only another reflected diffracted order is present that we have indicated in Fig. 10 as -1R(-1R)which has the same angle as the initial incident ray (I).

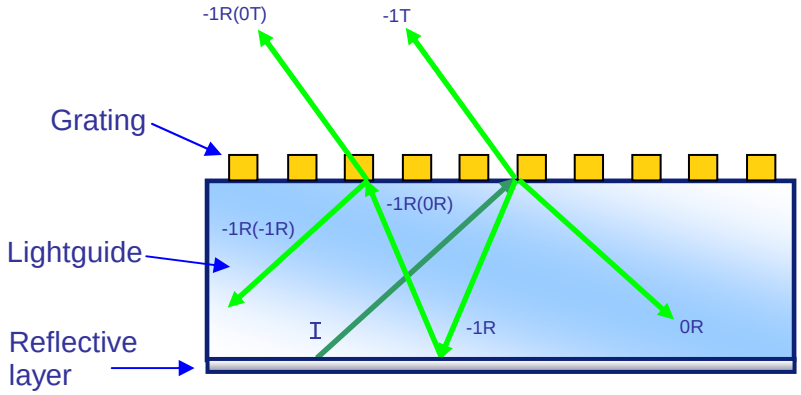

Fig. 10. Rays inside the lightguide. The incident beam I is partly reflected by the grating (0R), partly diffracted in transmission (-1T) and partly diffracted in reflection (-1R). The diffracted reflected beam is reflected once more at the reflective layer put on the base of the lightguide and comes again to the grating (-1R(0R)). It diffracts in reflection again by the grating (-1R(-1R) into the same direction as the incident beam I. This behavior is verified for every beam I with incidence angle in the interval $48°<\theta_{inc}<90°$ and for every wavelength of interest.

The lens array that is needed to image the colors on the appropriate pixels needs to match exactly to the pixel structure of the LCD panel and the angular distribution of the light extracted from the light guide by the grating. The geometry is sketched in Fig. 11. The sub-pixel pitch is denoted by *p*, the focal length of the lenses by *f*, and the width of the lenses by *D*.

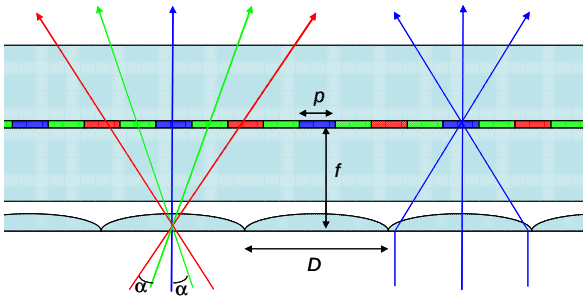

Fig. 11. Geometry of the lens array in front of the pixels.

If we assume that the grating spacing is chosen such that blue is emitted along the normal, and that the angle between the green and blue rays is roughly equal to the angle between the red and green rays, and that both angles are equal to α, the following equations apply to the lens parameters:

$$D = 4p\ ; \quad f = \frac{p}{\tan\alpha}\ ; \quad f_{\#} = \frac{f}{D} = \frac{1}{4\tan\alpha}$$

#84201 - $15.00 USD Received 18 Jun 2007; revised 2 Aug 2007; accepted 2 Aug 2007; published 6 Aug 2007

This shows that the width of the lenses is completely determined by the pixel spacing of the display. The strength, or focal length, is determined both by the pixel spacing of the display and by the angular range of the colors extracted from the light guide. The angular range is mainly determined by the grating spacing. Using an average value of $\alpha = 15°$, this implies an f-number of only 0.93. Hence the lenses need to be extremely strong. For thin lenses in air the focal length is related to the refractive index n and the radius of curvature R via the well known lensmaker's equation:

$$f = \frac{1}{n-1} R$$

However, for the strong lenses required here spherical aberrations will play an important role. Therefore we used ray-tracing simulations of the lens geometry in order to find the proper radius of curvature for the required focal length. In these simulations we also took the refraction by the glass substrate of the display into account. Our target display has a pixel pitch of 207μm, and therefore the pitch of the lens array is chosen to be 4 x 207 = 828μm. The total thickness of the panel, including polarizer foils, was measured to be 2.2mm.
Based upon our simulations a lens array was made with a radius of curvature of the lenses of 543μm, and a refractive index of 1.57. The lens array needs to be placed in close contact with the display in order to be close enough to focus the color lines on the position of the pixels within the LCD panel.

4. Evaluation of the backlight system

The experimental testing of the backlight system has been performed in several steps. At first we characterized the angular distribution of light outcoupled from the grating with an EZContrast 160 conoscope from Eldim S.A.[15]. The lightguide with the grating on top was placed in a side-lit configuration with a cold-cathode fluorescence lamp (CCFL) and a mirror at the other end of the lightguide. Results of this analysis are reported in Fig. 12 and clearly confirm the idea sketched in Fig. 5: a pattern of colors symmetric around zero azimuthal angle can be observed.

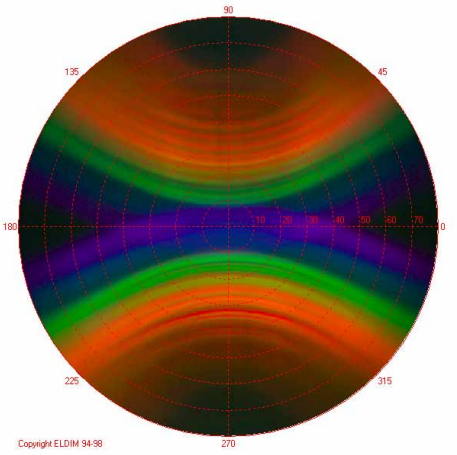

Fig. 12. Measurement of angular distribution of the light outcoupled from the grating. Some color overlap can be observed in the picture as predicted in Fig. 9(a).

Colors vary, from bottom to top, passing by red, green and dark blue and again green and red. Some overlap is however present between red and green and green and blue and it shows up with hybrid tonalities. This qualitatively corresponds to the results of Fig. 9(a).
The second measurement was with the microlens array in front of the grating. A picture of the resulting color distribution has been taken by a CCD camera and it is shown in Fig. 13(a). We

#84201 - $15.00 USD Received 18 Jun 2007; revised 2 Aug 2007; accepted 2 Aug 2007; published 6 Aug 2007

observe a periodical sequence of colored stripes that is to be imaged by the system (grating + microlens array) onto the diffuser in front of the LC layer. At this stage, the width of the various stripes is not exactly the same for all the colors. This is probably due to a not perfect focal strength of the microlens array used for the experiment and to an unequal spacing of wavelengths of the light source. We analyzed the pattern of Fig. 13(a) in order to measure how wide the gamut of our display could be. The obtained graph (Fig. 13(b)) shows several groups of points that mainly correspond to the peaks present in the spectral range of our light source (Fig. 13(c)). The dashed triangle represents the gamut of a common LCD-TV display. By comparing the triangle to our result we notice that the red peak (λ=615nm) is in our case absent. This is due to the color overlap between red and green already evidenced in Figs. 9, 12. The main result of this overlap is the orange color that we observe in the periodical structure of Fig. 13(a).

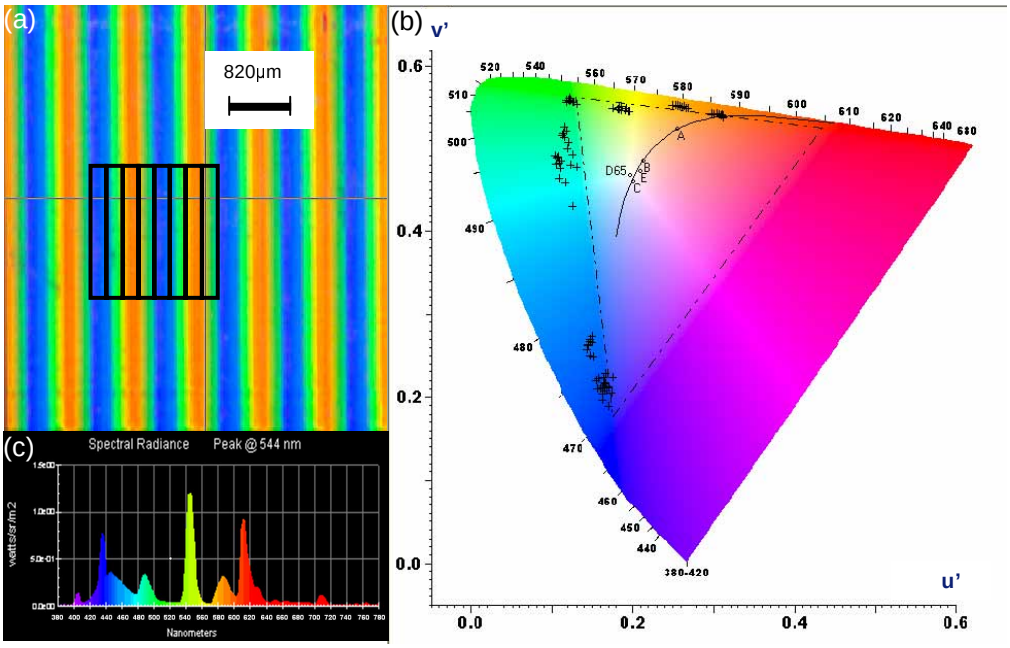

Fig. 13. (a). Photograph of periodically striped pattern as produced by a microlens array put in front of the grating. The image shows the RGBGR sequence of stripes. (b). Gamut of the obtained display. Several groups of points correspond to the peaks present in the spectral range of our light source. The dashed triangle represents the gamut of a common LCD-TV display. (c). Spectrum of a CCFL lamp.

5. Conclusions

Holographic diffraction gratings are very flexible optical elements that can be designed for a large range of applications. In this paper we have considered the realization of a grating for display applications. If the grating is used as a color-separating element, color-filters in front of the LC layer of the display can be avoided and the obtained configuration is very efficient. Several simulations have been performed to identify the features of the grating needed for obtaining best performances. Results show that period and depth are key-parameters. We realized a grating with a period of Λ=320nm and depth of L=210nm. This structure diffracts light coming from opposite directions into a symmetric RGBGR ray pattern. If a microlens array is put in front of the grating, the colored rays can be imaged onto the LCD with a periodically striped sequence forming a new pixel structure. A first prototype using this concept has been realized and its performance has been analyzed. The results confirm the

#84201 - $15.00 USD Received 18 Jun 2007; revised 2 Aug 2007; accepted 2 Aug 2007; published 6 Aug 2007

usability of the RGBGR pixel structure but unfortunately the color gamut of this system is not yet perfect because of some overlap between colored rays coming from the grating. Of course, color filters could be used to clean up the colors in which case the efficiency of the backlight would still be much better than without color separation. Alternatively, this issue can be resolved more efficiently by reducing the angular range of the light coming to the grating from the lightguide.

#84201 - $15.00 USD Received 18 Jun 2007; revised 2 Aug 2007; accepted 2 Aug 2007; published 6 Aug 2007